A Modified Imidazole as a Novel Latent Curing Agent with Toughening Effect for Epoxy

Kunxiang Shi, Yucai Shen,[*] Yuwei Zhang and Tingwei Wang[*]

α, β-unsaturated diester was used to react with secondary amine in imidazole ring and also restrain its reactivity. The modified imidazole would thermally decompose into imidazole and unsaturated diesters. Mixture of the latent curing agent with epoxy resins has long storage stability at room temperature for more than one month. The curing behavior of modified imidazole/epoxy was investigated by nonisothermal differential scanning calorimetry method and the curing kinetics results revealed that the modified imidazole has higher curing temperature but similar apparent activation energy. Furthermore, the modified imidazole brings better impact strength for cured epoxy.

1. Introduction

With the rapid development of semiconductor manufacturing industry and integrated circuit industry, epoxy resins are widely used as electronic packaging base materials because of their excellent insulating characteristics, outstanding chemical resistance and functionality.[1-4] In order to simplify the production processes and enhance the level of automation, one-component epoxy resin has been used in producing the epoxy molding compounds. However, when epoxy was mixed with curing agents, it will slowly solidify and the viscosity of the mixture will increase. This will result in poor fluidity and negative effects for production. Under current conditions, the one-component epoxy resin must be kept in cold storage to slow down the curing speed. To solve this problem, latent curing agent will be the key factor.[5,6] Latent curing agents often have very low reactivity with epoxy resins at room temperature but could rapidly solidify the epoxy resins when certain heat, light or pressure appears. In addition, they should not impair the performance of cured material. Based on this principle, many kinds of latent curing agents have been developed, such as imidazole derivatives,[7-9] dicyandiamide,[10,11] boron-amine complexes[12,13] and others.[14-16]

Imidazole derivatives account for most of latent curing agents, because they can provide polymers with better heat resistance, lower tensile elongation, higher modulus and wider range of cure temperature than amine-cured system. They play an important role in electronic integrated circuit encapsulation industry. Unmodified imidazole curing agents are less stable and the curing process occurs fast at room temperature. Generally, there are three usual modification methods to turn it into latent curing agent. The first one is to encapsulate imidazole curing agents in other materials.[17-22] The second one is to substitute the active hydrogen in secondary amine.[23-26] The third one is to restrain the reactivity of tertiary amine through various chemical bonds[7,27] or steric effects.[5] The first approach is to encapsulate curing agents in polymer materials such as polystyrene, poly(glycidyl methacrylate) and so on. They are designed to release imidazole curing agents when broken by melted or relaxation. However, microcapsules are powder-type agents, and they cannot be thoroughly mixed with liquid epoxy resin. Besides, the remaining wall material would affect the physical and mechanical performances of epoxy resins. The second way is to provide the 1-substituted imidazole derivatives as novel latent curing agents. They usually contain the strong withdrawing groups or bulky protecting groups, which would lower the reactivity of imidazole at room temperature. The third method is to restrain the reactivity of tertiary amine through metal-organic coordination bond or hydrogen bond. The latent curing agents made through the latter two methods are powder or liquid, and the addition of groups to the polymer systems does not have an adverse effect on properties of cured substance. By comparison, using various chemical bonds to restrain the reactivity of secondary amine or tertiary amine is more practical.

Compared to using other chemical bonds to restrain the reactivity of secondary amine, the chemical construction of α, β-unsaturated diesters can ensure the appearing of retro-Michael addition reaction and releasing the reaction of imidazole at high temperature. Arimitsu and coworkers have prepared kinds of these curing agent.[9,26] Thermal decomposition points and curing temperature were studied in their papers. However, the curing behavior and related thermal and mechanical properties of cured epoxy resin are not studied further, and those properties are very concerned for many applications. A liquid-type 1-substituted imidazole derivative has been developed in this study. Commercially available diethyl fumarate was used to react with secondary amine in imidazole ring and restrain its reactivity. Curability and storage stability were studied, and the curing kinetics and physicochemical properties of imidazole before and after the modification were also investigated.

2. Experimental
2.1. Chemical materials

College of Materials Science and Engineering, Nanjing Tech University, Nanjing, Jiangsu, 210009
E-mail: *ycshen@njtech.edu.cn; wangtw@njtech.edu.cn*
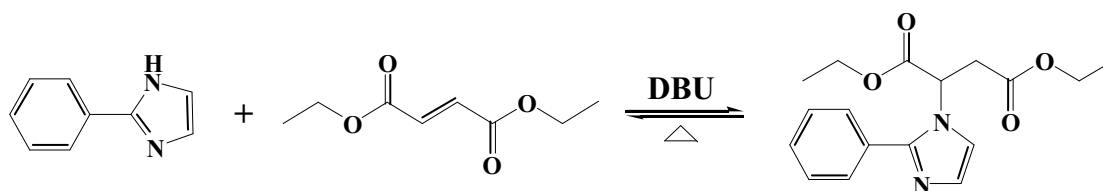
Scheme 1. Mechanism of Michael addition reaction and thermal decomposition.

Commercially available starting materials were used as purchased. Bisphenol-A diglycidyl ether (E-51), (epoxy equivalent 185, viscosity 2.5 Pa·s at 40 °C), purchased from Nantong Xingchen Synthetic Material Co., Ltd. was used. Diethyl fumarate (DF), 1,8-Diazabicyclo [5.4.0]-7-undecene (DBU), 2-phenylimidazole (PZ) were purchased from Aladdin Industrial Corporation. Petroleum ether (AR, 60 °C - 90 °C) and ethyl acetate (AR) were purchased form Wuxi Yasheng Chemical Co., Ltd. Acetonitrile (AR) was purchased from Sinopharm Chemical Reagent Corporation. Silica gel for column chromatography was from Shanghai Shengya Chemical Co., Ltd, and silica plates were from Yantai Jiangyou Co., Ltd.

2.2. Synthetic procedure of latent curing agent
The molecular design of latent curing agent, which has a succinate moiety, is shown in Scheme 1.

DBU (0.10 g, 0.7 mmol) was added to a mixture of PZ and DF in dry acetonitrile (10 mL). Different reactant ratios were tried, and an optimized reaction condition was chosen. The target product was successfully obtained with a yield of 69% as a brown viscous liquid (0.44 g) when 2 mmol PZ and 5 mmol DF reacted at 45 °C for 24 h. After the reaction and evaporation, the residue was purified using column chromatography on silica gel with petroleum ether/ethyl acetate (2/1, v/v) to get the modified 2-phenyl imidazole with diethyl fumarate (PZDF).

2.3. Characterization of product
Fourier transform infrared spectra (FTIR) were generated on Nexus 670 Fourier transfer infrared spectrometer (KBr pellets). H-nuclear magnetic resonance spectra (^{1}H NMR) were obtained using an AV400D nuclear magnetic resonance with CDCl$_3$ as solvent.

The thermal analysis of PZDF was performed using a simultaneous thermal analyzer STA449F (DSC-TG) from 40 to 300 °C under nitrogen atmosphere. The heating rate of scanning runs was 10 °C/min. To confirm the thermal decomposition products, TG-FTIR analysis was also used. Curing of PZ/E-51 and PZDF/E-51 were studied via DSC at a heating rate of 2.5, 5, 10, 15 °C/min, respectively. The mole ratio of curing agent to epoxy was 1/4.

For the measurement of pot-life, PZ and PZDF were respectively used as curing agent and the curing agent level was set to 1/40 (mol/mol) to epoxy. The samples were mixed at high agitation speed and degassed in vacuum oven. All samples were stored in glass beakers at 25 °C. The viscosity of the samples was measured periodically for one month by use of a rotary viscometer (NDJ-1) and the test was performed at 25 °C.

Dynamic mechanical analysis (DMA) was performed on a MCR302 instrument at a heating rate of 5 °C/min to measure the glass transition temperature of materials. The rectangular samples (25 mm × 6 mm × 2 mm) were loaded in the torsion mode at a frequency of 1 Hz under air atmosphere. PZ/E-51 samples were cured at 100 °C for 2 h and then at 160 °C for 4 h. PZDF/E-51 samples were cured at 140 °C for 2 h and then at 160 °C for 4 h. The mole ratio of curing agent to epoxy was 1/4.

The impact strength of cured specimens (4 mm × 10 mm × 100 mm) was obtained using a Charpy impact tester at room temperature. The cured process is the same with samples for DMA test.
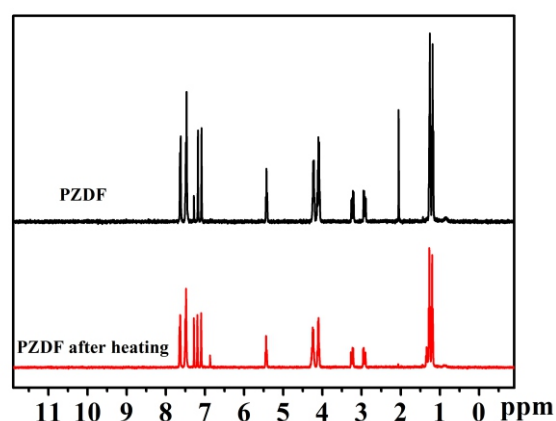
3. Result and discussion
3.1. Synthesis of PZDF
FTIR transmission spectrums of DF and PZDF are shown in Fig. 1. It can be seen that PZDF shows distinct characteristic peaks of benzene at
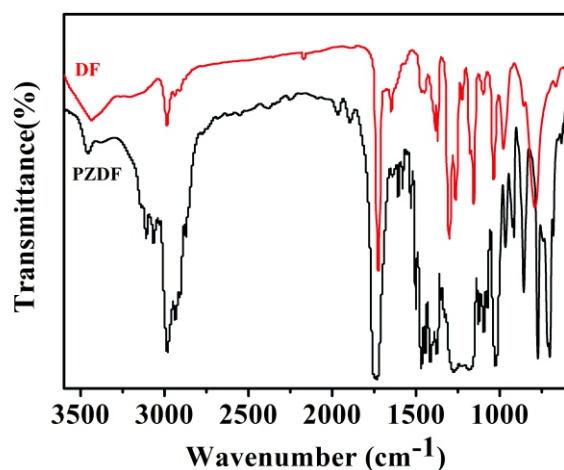
Fig. 1 FTIR transmission spectrums of DF and PZDF.

Fig. 2 ^{1}H-NMR spectra of PZDF before and after heating at 150 °C for 1 h.

3108cm^{-1}, 3066cm^{-1} (C-H, stretching vibration), 1605 cm^{-1}, 1578 cm^{-1}, 1501 cm^{-1}, 1445 cm^{-1} (benzene skeleton, stretching vibration), and 772 cm^{-1}, 701 cm^{-1} (C-H bonds of monosubstituted benzene, bending vibration). Besides, the characteristic peak of C=O group in PZDF move to the higher wavenumber (from 1724 cm^{-1} to 1732 cm^{-1}). This spectral change indicates the disappearance of adjacent double bond. ^{1}H NMR has further confirmed the chemical structure of PZDF (Fig. 2): δ 7.63 (d, J = 7.1 Hz, 2H, Ar–H), 7.48 (d, J = 6.8 Hz, 2H, Ar–H), 7.18 (s, 1H, Ar–H), 7.09 (s, 1H, =CH-N), 5.43 (t, J = 7.3 Hz, 1H, =CH-N), 4.35–3.96 (m, 4H, -OCH$_2$-), 3.23 (dd, J = 16.8, 7.1 Hz, 1H, O=C-CH$_2$-), 2.92 (dd, J = 16.7, 7.4 Hz, 1H, O=C-CH$_2$-), 2.05 (s, 1H, O=C-CH-), 1.43–1.01 (m, 6H, -CH$_3$).

3.2. The thermal decomposition study of PZDF

It is expected that the C-N bond formed in synthesis would restrain the nucleophilicity of the imidazole at room temperature but break at a higher temperature to cure epoxy, as shown in scheme 1. To examine the reversibility of the C-N bond, DSC-TG was used. As shown in Fig. 3a, two decalescence peaks appear in the DSC curve of PZDF and peak temperatures are 244 °C and 276 °C. The decalescence peaks appearing in the DSC curve include endothermic decomposition and endothermic gasification. At first, decomposition and gasification exist together. But there is only gasification in the latter period, and the decalescence rate decreases. The mass of PZDF begins to decrease with the endothermic at about 202 °C ($T_{5\%}$). Moreover, the varying tendencies of mass loss rate could be seen according to its TG and DTG curves (Fig. 3b). During the course of heating, the change of mass falls into two parts. The mass begins to decrease at about 202 °C. And at 250 °C, it turns into a lower speed with remains. This is due to the different boiling

points or decomposition temperatures of DF and PZ. The initial decomposition temperature, 202 °C, is caused by the boiling point of DF (214 °C). TG-FTIR analysis (Fig. 3c) shows that different compounds are released at different temperature. In the early stage, there is only carbon dioxide. At 228 °C (about the 19th minute), a peak at 1742 cm^{-1} (C=O, stretching vibration) appears, along with infrared characteristic peaks of C-H group (3987cm^{-1}, 1296cm^{-1} and 1257 cm^{-1}). This indicates that DF can be detected at 228 °C. This change agrees with the result from DSC-TG curves.

To confirm the thermal decomposition products, PZDF was heated in a tube at 150 °C for one hour and then was monitored by ^{1}H-NMR spectroscopy. Comparing the sample with PZDF (see Fig. 2), it is shown that the peak assigned to olefin protons of DF appeared at 6.87 ppm after heating. While the peak assigned to methine proton almost disappeared at 2.05 ppm and the peak assigned to methylene next to the carbonyl group was slightly decreased at 2.92 ppm and 3.23 ppm. This suggests the formation of DF with the decrease of PZDF in the course of heating. The spectral change proved that PZDF would be thermally decomposed into DF and PZ via a retro-Michael addition reaction, as shown in Scheme 1.

3.3. The curing behavior of E-51 with PZDF

The curing behaviors of PZ/E-51 and PZDF/E-51 systems were studied by nonisothermal DSC method. Fig. 4 shows the DSC curves for these systems at different heating rates. Under the same heating rate, the exothermic peak temperature (T_p) of PZDF/E-51 system moves toward a higher temperature compared to that of PZ/E-51 system, illustrating that PZDF reacts with epoxy at a higher temperature. Table 1 shows the T_p and total heat of PZ/E-51 and PZDF/E-51 systems at the heating rate
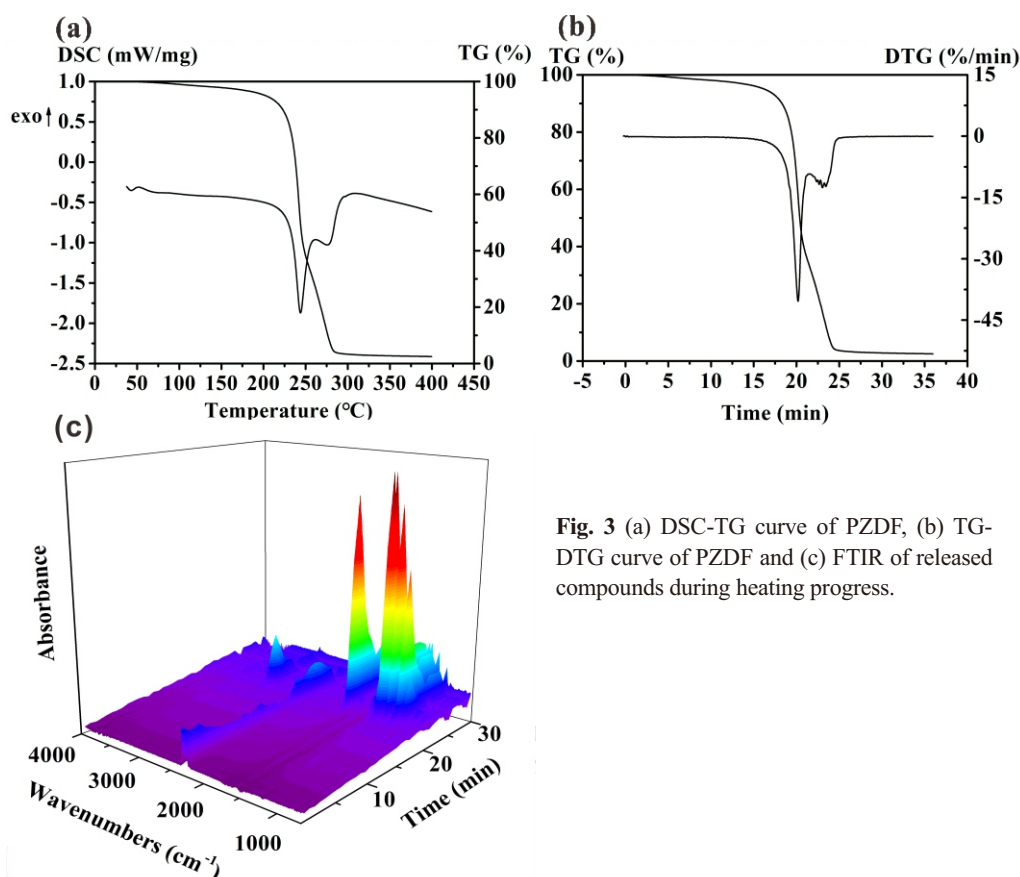

Fig. 3 (a) DSC-TG curve of PZDF, (b) TG-DTG curve of PZDF and (c) FTIR of released compounds during heating progress.

of 10 °C/min. It is clear that curing temperature increases from 125 °C to 146 °C after modification. As shown in Fig. 3a, the thermal decomposition temperature of pure PZDF is about 244 °C. However, the curing temperature is about 146 °C when PZDF is mixed with epoxy. There are two reasons for this difference. Firstly, for this thermal decomposition reaction, there is an equilibrium between reactants and products during the heating progress. The decomposed product PZ will react with epoxy rapidly when epoxy resin exists. The decrease of PZ will deeply promote the decomposition reaction and led to lower curing temperature. Besides, the tertiary amine in imidazole ring may act as anionic initiator and decrease the curing temperature too.[28] The DSC curve of PZ/epoxy shows two peaks. As shown in Scheme 2, the first peak corresponded to the first and the second adduct reactions of epoxy resin and imidazole. The 1:1 adduct and the 1:2 adduct are created in this stage. The second peak is caused by the anionic polymerization of the epoxy resin from the 1:2 adduct. This action needs higher temperature. The first peak and the second peak merge for PZDF/epoxy
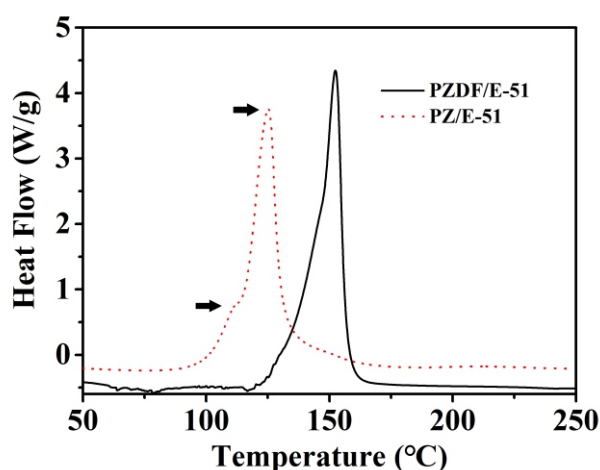

Fig. 4 DSC curves of epoxy with PZ and PZDF.

because the temperature of the adduct reaction is very close to the temperature of the polymerization.[29,30] This also confirms that PZDF begin to react with epoxy at a higher temperature because of the restraint of reactivity. In Table 1, the values of total exothermic heat were 350 J/g for PZ/epoxy and 287 J/g for PZDF/epoxy. The latter was slightly lower than the former. E-51/PZDF shows a lower value due to the heat absorption in its decomposition and evaporation process.

The apparent activation energy of PZ/E-51 and PZDF/E-51 systems was determined using Kissinger and Ozawa methods, respectively. The kinetic parameters can be obtained from Kissinger and Ozawa methods. Kissinger method can be expressed as the following Eq. (1):

$$\ln\left(\frac{\beta}{T_P^2}\right) = \ln\frac{AR}{E_1} - \frac{E_1}{R} \cdot \frac{1}{T_P} \qquad (1)$$

Where β is the heating rate, R is universal gas constant, A is the Arrhenius constant, and E_1 is the apparent activation energy simulated by Kissinger method. Therefore, the value of E_1 can be calculated from the slope of the linear fitting plot of $\ln(\beta/T_p^2)$ versus $1/T_p$. Ozawa method can be expressed as Eq. (2):

$$\frac{d(\log\beta)}{d(\frac{1}{T_P})} = -0.4567\frac{E_2}{R} \qquad (2)$$

Where E_2 is the apparent activation energy obtained from Ozawa method, and it can be obtained from the slope of the linear fitting plot of $\ln\beta$ versus $1/T_p$. Furthermore, the reaction order (n) can be calculated using Crane equation as shown in Eq. (3):

$$\frac{d(\ln\beta)}{d(\frac{1}{T_P})} = -\frac{E}{nR} \qquad (3)$$

where E is the average apparent activation energy calculated from E_1 and E_2, and n is derived from the slope of $\ln\beta$ versus $1/T_p$.
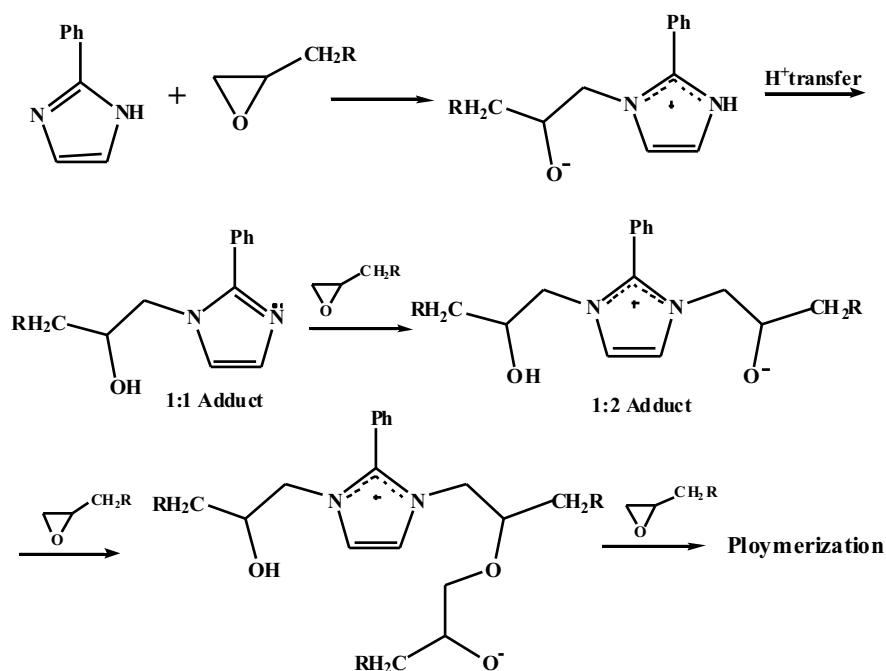
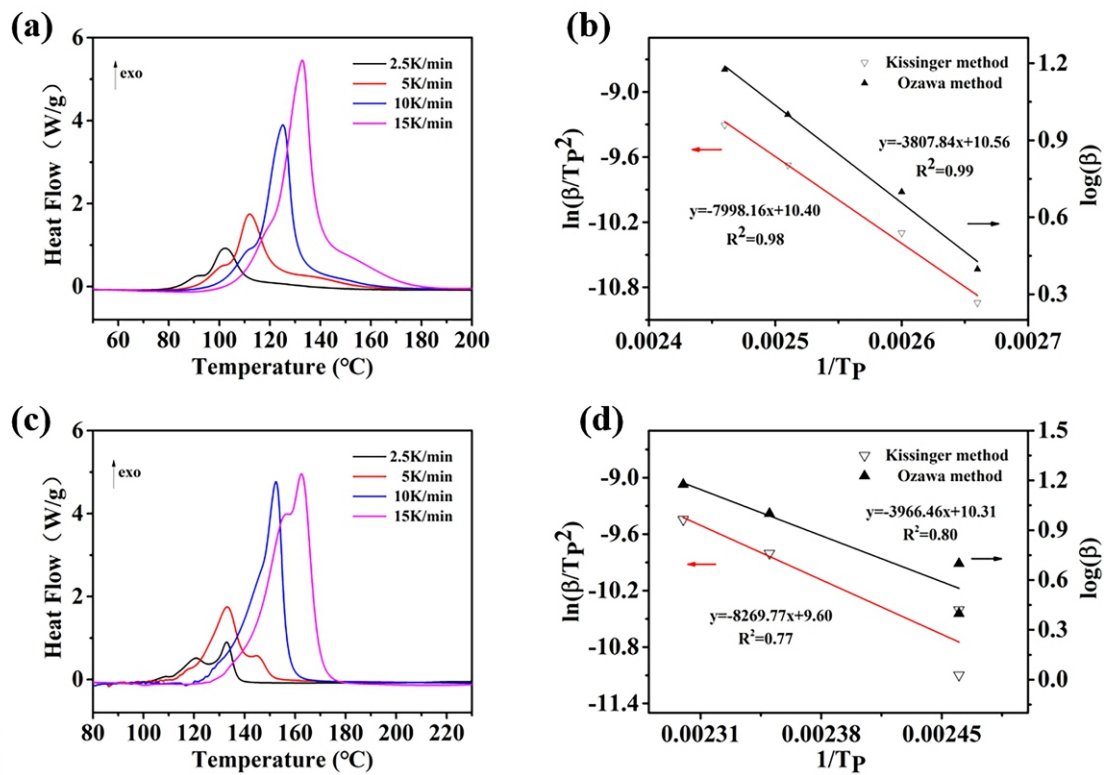**Scheme 2.** Curing mechanism of PZ with epoxy resin.

Fig. 5 DSC curves at different heating rates: (a) PZ/E-51; (c) PZDF/E-51; (b) fitting lines of PZ/E-51; and (d) PZDF/E-51 system through different methods.

Table 1. Curing Characteristics of Epoxy Systems.

Samples	$T_p(^{\circ}C)^{a}$	Total heat(J/g) [b]	E_1(kJ/mol)	E_2 (kJ/mol)	E (kJ/mol)	n
PZ/E-51	125	350	67.62	70.48	69.05	0.93
PZDF/E-51	146	287	66.83	70.19	68.51	2.14

Note: a: the exothermic peak temperature at the heating rate of 10 $^{\circ}$C/min
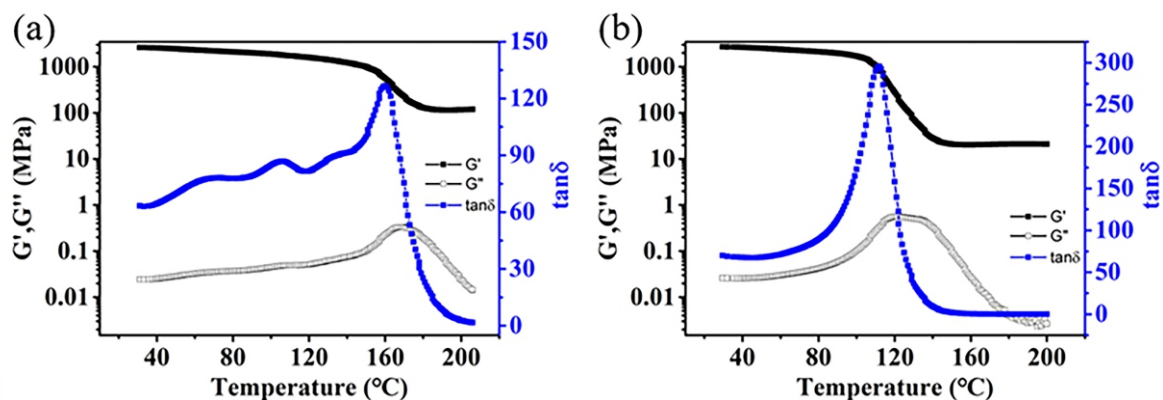b: the total heat at the heating rate of 10 $^{\circ}$C/min

Fig. 6 Storage modulus (G'), loss modulus (G") and damping factor (tan δ) of epoxy cured by (a) PZ and (b)PZDF

Fig. 5(a), (c) show the DSC curves of PZ/E-51 and PZDF/E-51 composite at different heating rates, respectively. The heating rate was 2.5, 5, 10, 15 K/min. The fitting results were shown in Fig. 5(b),(d), according Eq. (1), (2), and all the obtained results were summarized in Table 1. The calculated E value for PZ/E-51 is 69.05 kJ/mol, which is close to that of PZDF/E-51 (68.51 kJ/mol), indicating that they have similar reactivity when cured with E-51. In PZDF/E-51 system, the curing agent is also the free imidazole released from retro-Michael addition reaction. Furthermore, the calculated n value for PZDF/E-51 is 2.14, which is much higher than that of PZ/E-51 (0.93). The curing of PZ/E-51 system is approximately a first-order reaction and that of PZDF/E-51 system is approximately a second-order reaction. This means curing agent's concentration in PZDF/E-51 system affects the curing reaction more significantly than that in PZ/E-51 system. This may be caused by decomposition reaction.

3.4 Thermal and mechanical properties of epoxy blends.

T_g reflects the mobility of the chain segments and the temperature resistance for the thermosetting resins. Fig. 6 shows the curves of the DMA test for epoxy cured by different curing agents. The T_g is derived from the maximum peak temperature of tanδ curves. The peaks at 169 °C and 144 °C indicated the T_g values of the epoxy resin cured by imidazole and modified imidazole, respectively. It is clear that PZDF would significantly reduce the T_g of samples. The impact strength of PZDF/E-51 has a value of 5.2 kJ/m^2, which is much higher than that of PZ/E-51 (1.4 kJ/m^2). The results of the impact test are in agreement with the results of T_g. DF would be released during the retro-Michael addition reaction and act as a toughening agent. These prove that PZDF would increase the toughness of epoxy materials.

3.5. Measurement of pot-life.

The storage stability of these compositions was further evaluated by measuring their changes of viscosity at 25 °C (Fig.7). The viscosity of epoxy mixed with PZ significantly increases from 20 Pa·s to 43 Pa·s in 5 days, indicating that PZ exhibits poor latency properties at room temperature. For epoxy mixed with PZDF, the viscosity remains under 20 Pa·s within 27 days and keeps the low viscosity for more than one month. The viscosity of epoxy mixed with PZDF is much lower than epoxy itself, which is due to the addition of the liquid curing agent. These results indicate that PZDF has superior latency properties than PZ at room temperature. In addition, the modified imidazole would also reduce viscosity to get good maneuverability.
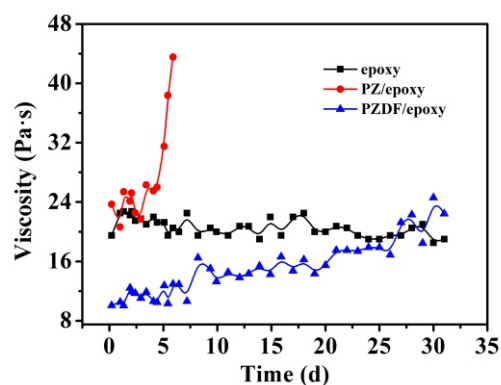

Fig. 7 Diagram of the viscosity of epoxy treated with different curing agent against storage time at 25 °C.

4. Conclusions

In this work, a novel liquid-type latent curing agent PZDF was successfully developed. α,β-unsaturated diesters was used to react with secondary amine in imidazole ring and restrained its reactivity.

Compared with PZ/E-51, the curing temperature of PZDF/E-51 increases from 125 °C to 146 °C. The apparent activation energies of PZ/E-51 and PZDF/E-51 systems were determined using Kissinger and Ozawa methods, respectively. The calculated E values for two systems are close, indicating that they have similar reactivity during curing. Furthermore, the calculated n value indicates that the curing of PZ/E-51 system is approximately a first-order reaction and that of PZDF/E-51 system is approximately a second-order reaction. The T_g value of the epoxy resin cured by modified imidazole reduces from 169 °C to 144 °C, but the impact strength increases from1.4 kJ/m^2 to 5.2 kJ/m^2. PZDF would increase the toughness of samples. PZDF can prevent curing reactions to some extent at low temperature but would recover its reactivity via a retro-Michael addition reaction at high temperature. Epoxy resin mixed with PZDF would have long-term storage stability at room temperature, for more than one month. This type of thermal latent curing agent may have good potential as electronic packaging materials, such as epoxy molding compounds without frozen transportation.

Conflict of interest

There are no conflicts to declare.

Acknowledgements

References

1. L. Guadagno, M. Raimondo, V. Vittoria, L. Vertuccio, C. Naddeo, S. Russo, B. Vivo, P. Lamberti, G. Spinelli and V. Tucci, *RSC Adv.*, 2014, **4**, 15474-15488.
2. J. Gu, X. Yang, Z. Lv, N. Li, C. Liang and Q. Zhang, *Int. J. Heat Mass Transfer*, 2016, **92**, 15-22.
3. S. J. Park, M. K. Seo, J. R. Lee and D. R. Lee, *J. Polym. Sci. Pol. Chem.*, 2001, **39**, 187-195.
4. Y. Zhang, Y. Shen, K. Shi, T. Wang and E. Harkin-Jones, *Composites Part A*, 2018, **110**, 62-69.
5. K. Kudo, S. Fuse, M. Furutani and K. Arimitsu, *J. Polym. Sci. Pol. Chem.*, 2016, **54**, 2680-2688.
6. K. Suzuki, H. Horii, Y. Sugita, F. Sanda and T. Endo, *J. Appl. Polym. Sci.*, 2004, **94**, 961-964.
7. K. Kudo, M. Furutani and K. Arimitsu, *ACS Macro. Lett.*, 2015, **4**, 1085-1088.
8. K. Chen, Y. Shen, M. Yeh and F. F. Wong, *J. Taiwan Inst. Chem. E*, 2012, **43**, 306-312.
9. K. Arimitsu, S. Fuse, K. Kudo and M. Furutani, *Mater. Lett.*, 2015, **161**, 408-410.
10. L. Feng, Y. Wang, Y. Wang, H. Liu and J. Zhao, *J. Appl. Polym. Sci.*, 2013, **127**, 1895-1900.
11. Y. C. Wang, S. D. Lin, Y. Y. Tu, J. H. Li, J. W. Hu and F. Li, *Fine Chem.*, 2016, **33**, 224-230.
12. S. Liu, J. Chen, J. Zhao, Z. Jiang and Y. Yuan, *Polym. Int.*, 2015, **64**, 1182-1190.
13. C. Martin, G. Lligadas, J. C. Ronda, M. Galia and V. Cadiz, *J. Polym. Sci., Part A: Polym. Chem.*, 2006, **44**, 6332-6344.
14. Y. R. Ham, D. H. Lee, S. H. Kim, Y. J. Shin, M. Yang and J. S. Shin, *J. Ind. Eng. Chem.*, 2010, **16**, 728-733.
15. S. L. Xing, J. S. Yang, Y. L. Huang, Q. Zheng and J. C. Zeng,

Mater. Design., 2015, **85**, 661-670.

16. J. Wang, Y. Z. Xu, Y. F. Fu and X. D. Liu, *Sci. Rep.*, 2016, **6**, 1-7.

17. Y. Q. Shi, Q. Y. Zhang, A. J. Ma and C. J. Yin, *Chem. Bull.,* 2012, **75**, 245-250.

18. Y. Q. Shi,Q. Y. Zhang, Y. N. Yin, B. L. Zhang and J. W. Gu, *CIESC. J.*, 2011, **62**, 2651-2656.

19. J. Fan, Y. Zheng, Y. Xie, Y. Sun, Y. Luan, W. Jiang, C. Wang, S. Liu and X. Liu, *Compos. Sci. Technol.*, 2017, **138**, 80-90.

20. C. Li, J. Tan, J. Gu, Y. Xue, L. Qiao and Q. Zhang, *Compos. Sci. Technol.*, 2017, **142**, 198-206.

21. D. A. Unruh, S. J. Pastine, J. C. Moreton and J. M. J. Frechet, *Macromolecules*, 2011, **44**, 6318-6325.

22. Y. J. Shin, M. J. Shin and J. S. Shin, *Polym. Int.*, 2017, **66**, 795-802.

23. F. F. Wong, K. Chen, C. M. Lin and M. Yeh, *J. Appl. Polym. Sci.*, 2007, **104**, 3292-3300.

24. W. Yen, K. Chen, M. Yeh, N. Uramaru, H. Lin and F. F. Wong, *J. Taiwan Inst. Chem. E*, 2016, **59**, 98-105.

25. D. Lei, W. Ma, L. Wang and D. Zhang, *J. Appl. Polym. Sci.*, 2015, **132**, 42563-42572.

26. K. Kudo, M. Furutani and K. Arimitsu, *J. Polym. Sci. Pol. Chem.*, 2016, **54**, 3411-3414.

27. H. Maka, T. Spychaj and R. Pilawka, *Ind. Eng. Chem. Res.*, 2012, **51**, 5197-5206.

28. M. Ghaemy and S. Sadjady, *J. Appl. Polym. Sci.*, 2006, **100**, 2634-2641.

29. Y. R. Ham, S. H. Kim, Y. J. Shin, D. H. Lee, M. Yang, J. H. Min and J. S. Shin, *J. Ind. Eng. Chem.*, 2010, **16**, 556-559.

30. V. Jisova, *J. Appl. Polym. Sci.*, 1987, **34**, 2547-2558.